Influence of Assimilation of Subsurface Temperature Measurements on Simulations of Equatorial Undercurrent and South Equatorial Current Along the Pacific Equator

David Halpern[1], Ming Ji[2], Ants Leetmaa[2], Richard W. Reynolds[2]

[1] Jet Propulsion Laboratory
California Institute of Technology
Pasadena, CA 91109-8099

[2] National Centers for Environmental Prediction
National Oceanic and Atmospheric Administration
Camp Springs, MD 20742

16 December 1997

Abstract

Equatorial Pacific current and temperature fields were simulated with and without assimilation of subsurface temperature measurements for April 1992- March 1995, and compared with moored buoy and research vessel current measurements. Data assimilation intensified the mean east-west slope of the thermocline along the equator in the eastern Pacific, shifted eastward the longitude of the mean Equatorial Undercurrent (EUC) maximum speed 800-km to 125°W, and produced a 25% stronger mean EUC core speed in the eastern Pacific. In the eastern Pacific the mean EUC core speed simulated with data assimilation was slightly more representative of observations compared to that computed without data assimilated; in the western Pacific the data assimilation had no impact on mean EUC simulations.

Data assimilation intensified the north-south slope of the thermocline south of the equator in the western Pacific to produce a thicker and more intense westward-flowing South Equatorial Current (SEC) in the western Pacific. In the western Pacific the mean SEC transport per unit width simulated with data assimilation was more representative of observations compared to that computed without data assimilation. However, large differences remained between the observed SEC transport per unit width and that simulated with data assimilation. In the eastern Pacific, the data assimilation had no impact on mean SEC simulations.

The temporal variability of monthly mean EUC core speeds and SEC transports per unit width were increased significantly by data assimilation. It also increased the representativeness of monthly mean SEC transports per unit width to the observations. However, the data representativeness of monthly mean EUC core speeds was decreased. Results could be explained by the coupling between zonal gradient of temperature and EUC and between meridional gradient of temperature and SEC. Longitudinal variations along the Pacific equator of the impact of data assimilation on the EUC and SEC precludes the choice of a single site to evaluate the effectiveness of data assimilation schemes.

1 Introduction

In 1986, a method was developed at the United States National Meteorological Center, now National Centers for Environmental Prediction (NCEP), to operationally produce numerical simulations of monthly mean temperature and current fields throughout the tropical Pacific Ocean. In 1989, assimilation of subsurface temperature data was introduced into the NCEP hindcast-analysis system (Leetmaa and Ji, 1989) to correct errors caused by deficiencies in surface fluxes (especially wind stress) and parameterizations of subgrid-scale physical processes in the ocean general circulation model (OGCM). Enfield and Harris (1995), Ji and Smith (1995), and Ji et al. (1995) showed that assimilation of subsurface temperatures improved simulations of sea level and temperature. However, it is not a priori conclusive that NCEP simulations of upper-ocean current in the equatorial Pacific would similarly be improved. For instance, Hao and Ghil (1994), using a relatively simpler model than an OGCM, found that updating thermocline depth could increase the error of the simulated zonal current, even when data were assimilated everywhere at each time step. At NCEP, insertion of subsurface temperatures into the model ocean did not occur regularly in time nor at each grid-point, causing local variations of thermocline height and thickness. Resultant horizontal pressure gradient and, consequently, velocity would be altered compared to locations where no data were assimilated. In this paper, we examine the impact of subsurface temperature assimilation on the Equatorial Undercurrent (EUC) and South Equatorial Current (SEC) along the Pacific equator.

All simulations for the April 1992- March 1995 period were computed at NCEP, according to the method described by Ji et al. (1995) and Leetmaa and Ji (1996). The April 1992- March 1995 interval coincided with three warm episodes of the El Niño Southern Oscillation phenomenon (Goddard and Graham, 1997). Wind stress components were computed from the NCEP 6-hour, approximate 1.50-latitude x 1.50-longitude, 1000-mb operational surface wind analyses. We used 1 000-mb wind analyses, in which the height corresponded to about 40 m, because the operational 10-m height wind speeds were too low during this period. (The accuracy of NCEP 10-m wind analyses has since improved.) A constant drag coefficient (1.25x10-3) was used. Monthly mean wind stress components were calculated from 6-hour stresses.

Two kinds of subsurface temperature data were assimilated. Expendable bathythermographs (XBTs) dropped from ships and Tropical Atmosphere-Ocean moored-buoy thermistor chains (McPhaden, 1995) provided NCEP with real-time subsurface temperature data via the global telecommunications system (GTS). Depths of XBT data were increased by 3% to correct for depth biases (Hanawa et al., 1995). The average number of XBT tneasurements between 10°S and 10”N in a typical 4-week interval, which was the influence time awarded to an XBT profile, was about 260. The XBT network was concentrated primarily along three shipping lanes that virtually excluded the 140°W -11 O°W area, where the zonal slope of the thermocline along the equator had its greatest magnitude. Thermocline information is important to the simulation of tropical ocean currents (Cane and Sarachik, 1979); we therefore note that the number of 10°S - 10ON real-time XBT data received at NCEP decreased by about 80% from April 1992 to March 1995. However, the effect was mitigated by the doubling of the number of TAO sites from 35 to 60, and the segment of the TAO army between 2°S and 2°N was essentially unchanged during this period. At each 1-hour assimilation time step, only about **5%** of the model l/30-latitude x 1.50-longitude grid regions within 10° of the equator were updated with subsurface temperature measurements. Simulations differed only whether there was or was not assimilation of subsurface temperatures. The velocity field was unconstrained by assimilation of temperature data.

Current measurements determined the representativeness of simulated currents, even though current measurements have errors themselves (e. g., Plimpton et al., 1997). Moored buoy current measurements were recorded at the equator by the Pacific Marine Environmental Laboratory at 165°E, 140°W and 110”W (McPhaden, 1995) and University of South Florida at 170°W (Weisberg and Wang, 1997). Currents at 165°E and 170°W were retrieved between 10 and 220 m at 5-m and 10-m intervals, respectively, with an acoustic Doppler current profiler (ADCP). At 140°W and 110”W current meters were placed at 10,25,45,80, 120, and 200 m. Record lengths at 165°E, 170°W, 140°W and 11 O°W were 29, 36, 36 and 34 data-months, respectively. A data-month was equal to 20 or more data-days within a calendar month. A 20-day minimum interval was dictated by the existence of large-amplitude 20-day current oscillations (Philander et al., 1985). Also, we used ADCP data recorded by the French research vessel *l'Atalante* along the equator from 166”E - 150°W during 9-19 October 1994 (Eldin et al., 1997).

2 Results

In the equatorial Pacific, the depth of the 20”C isotherm is used as an indicator of the thermocline because it occurs approximately within the center of the thermocline defined by the depth interval between the 25°C and 15°C isotherms. Assimilation of subsurface temperature data intensified the east-west slope of the 20°C isotherm by 25% from 140”W to 105°W (Figure 1). In no other longitudinal band of similar dimension had data assimilation produced a change in mean thermocline slope of similar magnitude. The thermocline change in the eastern equatorial Pacific was primarily caused by TAO data because of the rarity of XBT data in this region.

2.1 Equatorial Undercurrent

The eastward-flowing EUC has a maximum speed, named core speed, at about 75-150 m depth, depending on longitude and time of year. The core speed is a reasonable measure of the EUC because core speed and transport are correlated. At each moored-buoy site, the observed maximum eastward current was a good approximation of the core speed, including 140”W and 110”W because, based upon years of experience, a current meter had been placed at the approximate depth of the core speed. Simulated core speeds were determined from currents computed in 10-m layers in the uppermost 100 m and in approximate 20-m layers from 100-200 m. A core speed difference, whether between simulation and observation or between simulations, was arbitrarily defined to be significant if the difference was at least 10 cm s-’, because this value is easily detectable by measurements.

The impact of data assimilation on the mean EUC core speed was longitude dependent (Figure 2). In the western Pacific, differences in mean EUC core speed, whether between simulations or between simulation and observation, were smaller than 10 cm s^{-1}. A different situation ensued in the eastern Pacific. From 135°W - 95°W, data assimilation increased the mean core speed by more than 10 cm S-l and by as much as 25 cm S-*, and moved the mean position of maximum core speed 800 km eastward to 125”W. Maximum values of 10-200 m integrated eastward or EUC transport per unit width simulated with and without data assimilation were 160 and 110 m^2 S-*, respectively, and occurred at 125°W and 135°W, respectively. Had this difference been maintained in a north-south distance of ± 50 km of the equator, the EUC transports would have differed by 5x1 0^6 $m^3 s^{-1}$ (5 Sv) or about 25% of the typical EUC transport. These features reaffirm the strong association between variations of mean zonal slope of the thermocline (Figure 1) and mean EUC transport.

To a first approximation, the equilibrium EUC transport per unit width, T_{EUC}, is proportional to zonal wind stress, τ_x. The EUC represents a balance between vertically integrated accelerations caused by the east-west pressure gradient, $\rho^{-1}(\partial p/\partial x)$, where ρ is density and p is pressure and by the vertical gradient of the east-west component of internal friction, $\partial(\tau_{x,\ internal}/\rho)/\partial z$. With $(1/\rho)(\partial p/\partial x)$ represented by the east-west slope of sea level, $g\eta_x$, where g is gravity, then $g\eta_x = \tau_x/\rho H$, where H is mixed-layer depth. Therefore, $T_{EUC} \propto \eta_x$, and $\eta_x \propto$ zonal slope of the thermocline. Data assimilation produced a 25% increase in zonal slope of the thermocline (Figure 1) and, consequently, η_x would change by a similar amount, which resulted in 25% increase in mean EUC core speed (Figure 2) and 50% increase in mean EUC transport per unit width.

Insertion of subsurface temperature data increased the temporal variability of simulated currents (Figure 3), as expected because each subsurface temperature profile would alter the modeled horizontal temperature gradient to make it more consistent with natural conditions. The subsequent adjustment toward balance between horizontal gradient of temperature and current, characteristic of all data assimilation schemes, introduces Kelvin and Rossby wave motions and other current fluctuations with a wide variety of space and temporal scales. The effect of these adjustments are similar to those experience when initiating model forecasts from unbalanced initial conditions, also known as initialization shock. Wave and current fluctuations, produced as a result of initialization shock, are excited continuously during a simulation with data assimilation.

Of the four buoy sites, only at 140°W and 110”W did data assimilation increase the standard deviation of monthly mean EUC core speeds at least 10 cm s^{-1} (10 cm s^{-1} at 140°W and 13 cm s^{-1} at 110°W) compared to those computed from simulations made without data assimilation. At each of the four buoy sites, the root-mean-square (rms) difference computed between observed and simulated monthly mean EUC core speeds were the same, with 95% confidence, whether data had or had not been assimilated. A similar result was obtained for the correlation coefficients. However, the rms difference increased substantially towards the east, from 11 cm s^{-1} at 165°E to 28 cm s^{-1} at 11 O°W. At 11 O“W, data assimilation reduced agreement between observed and simulated standard deviations: without (with) data assimilation the difference in standard deviations was 1 (12) cm s^{-1}. Inspection of monthly mean EUC core speeds at 110”W (Figure 3D) shows core speeds simulated with data assimilation much too large during January - March 1993 and June - September 1994. Why the insertion of TAO data, as distinct from XBT data which occurred very infrequently in the eastern equatorial Pacific, over intensified the EUC at 100”W is unknown. Perhaps the data assimilation scheme overcompensated tropical instability wave amplitudes, which are especially large during these months (Philander et al., 1985) and which are not well simulated (Chen et al., 1994).

3.2 South Equatorial Current

Without data assimilation the mean SEC thickness was nearly uniform with longitude (Figure 4A), varying from 30 m in the west to 15 m in the east. With data assimilation the mean SEC thickness in the west reached about 100 m and was near zero in the east, which was similar to the longitudinal profile determined from moored-buoy current measurements (Figure 4A). Gouriou and Toole (1993) reported the 1984- 1991 mean SEC thickness at 165°E was 100 m, which was in much better agreement with the SEC thickness simulated with data assimilation than that computed without data assimilation (Figure 4A).

The SEC flow is analyzed with respect to the transport per unit width (Figure 4B). In the eastern Pacific, the mean SEC transports per unit width computed with and without data assimilation were similar and were smaller than observed values. A very weak SEC occurred at 140°W and 1 IO*W and throughout the 150°W - 10OOW longitudinal band. In the western Pacific, no satisfactory agreement was found between the two simulations. Our representation of the mean SEC computed without data assimilation was similar to that simulated by others (Philander et al, 1987; Schopf and Loughe, 1995). The 3.5-times increase in 150°E - 170°W mean SEC transport per unit width produced by data assimilation was so large as to cast doubt on its validity. Comparison of observed and simulated transports at the moored buoy sites did not resolve the situation. At 170°W the observed transport was virtually identical to that simulated with data assimilation, but at 165°E neither simulation had acceptable agreement with observed transport. In addition to having data assimilation increase the mean SEC thickness (Figure 4A), the simulated mean westward current at the surface increased, from 20 to 60 cm s^{-1} at the date line (not shown). Data assimilation raised the thermocline at the equator by a small amount and depressed it by 40 m at 6°S, enhancing the north-south slope of the thermocline (Figure 5), which at 3°S would enhance the geostrophic current by about 30 cm s-'. Thus, it seemed feasible for data assimilation to increase SEC transport per unit width by 15 m^2 s" 1 beyond the amount simulated without data assimilation, but this would not explain excessive mean SEC westward transports from 165°E - 180°E. It is a problem to simulate near-surface currents in the western equatorial Pacific, as also described by Acero-Schertzer et al. (1997). This warm pool region where rainfall exceeds evaporation by 1 m has complicated wind, current, hydrographic and ocean mixing structures (Wijesekera and Gregg, 1996).

To help determine reliability of the simulated SEC intensity in the western Pacific, the 9-19 October 1994 *l'Atalante* ADCP data were averaged in longitude and depth to correspond to the NCEP grid. The October 1994 SEC transports per unit width simulated without data assimilation were nearly uniform (- 5 m^2 S-l) throughout the 165°E - 150°W region. With data assimilation the simulated transports varied longitudinally, reached maximum (- 33 $m^2 s^{-1}$) at 173°E, and were in better agreement with *l'Atalante* observations to confirm that the SEC was significantly more intense west of 170°W (Figure 4C). Further evidence of a strong zonal gradient of SEC transport per unit width in October 1994 was provided with moored buoy current measurements, in which SEC transports per unit width were - 34 and -3 m^2s^{-1} at 165°E and 170°W, respectively (not shown). In contrast to the April 1992- March 1995 mean simulations, in October 1994 the observed SEC transports west of the date line, including 165°E, were significantly greater than those simulated with data assimilation (compare Figures 4B and 4C). Caution is advised in interpretation of a comparison between monthly mean OGCM simulations and data recorded over a 10-day interval from a moving ship because space and time fluctuations associated with each method are not separable. In the western Pacific, substantial upper-ocean current fluctuations are produced by episodic westerly wind bursts (Delcroix et al., 1993). Also, the NCEP data assimilation procedure (Ji et al., 1995), with a 4-week "utilization" time interval for subsurface temperature observations, reduced the influence of submonthly oceanographic phenomena.

That data assimilation increased the temporal vanability of monthly mean SEC transport per unit width was not surprising. At 165"E and 170°W the standard deviations of SEC transport without (with) data assimilation were 5 (14) and 7 (13) m^2 S-l, respectively. Differences between standard deviations computed from observations and simulations with data assimilation were less than 1 m^2s^{-1} at 165°E and 170°W, indicating a positive influence produced by data assimilation.

4 Conclusions and Discussions

Assimilation of subsurface temperature observations altered simulated currents along the equator in the Pacific. In the eastern (western) Pacific the mean EUC (SEC) was strengthened. Simulations of the mean EUC (SEC) in the eastern (western) Pacific made without data assimilation were less reliable than those computed with data assimilation. Data assimilation increased temporal variability of monthly mean EUC and SEC currents. Results could be explained by the coupling between zonal gradient of temperature and EUC and between meridional gradient of temperature and SEC. The increase in temporal variability produced with data assimilation did not agree with observations.

Our finding that the influence of data assimilation on upper ocean currents along the Pacific equator was longitude dependent suggests caution in evaluation of data assimilation schemes at a single location. For instance, current measurements at 140°W were used by Carton et al. (1996) to show how data assimilation, which involved altimeter sea surface topography measurements in addition to XBT and TAO subsurface temperature measurements and a different scheme from the one we employed, did not affect the May 1993- April 1994 mean SEC simulation. While this result was similar to ours, the situation was much different further to the west (Figure 4) where SEC simulations were affected by data assimilation. With respect to the mean EUC core speed at 140°W, Carton et al. (1996) found data assimilation increased it by 15 cm S-l compared to that computed without data assimilation. The mean EUC core speed that Carton et al. (1996) simulated with data assimilation was 40 cm s^{-1} smaller than that observed (100 cm s-l), and the difference was four times larger than our result (Figure 2). Also, inspection of Figure 3C shows very good correspondence between the May 1993- April 1994 observed mean EUC core speed (100 cm s^{-1}) and that simulated with data assimilation. In another example in which 140°W moored currents demonstrated effectiveness of a data assimilation scheme, Fukumori (1995) showed that data assimilation, which involved yet another scheme and also a different ocean model compared to those used by Carton et al. (1996) and ourselves, improved the agreement with respect to observations of temporal variability of 25-m zonal current. In our investigation, data assimilation also improved the representation of temporal variability of 25-m zonal current, with standard deviations of 3S monthly mean values equal to 23, 25, and 16 cm s^{-1} for observations, simulation with data assimilation, and simulation without data assimilation, respectively. Our “system” achieved a higher level of improvement compared to that determined visually from Fukumori’s (1995; plate 7) result.

Although currents simulated with data assimilation were more representative of observations, ample opportunities exist for further improvement. Several candidates are briefly discussed.

Although there is always a need to have more data to assimilate, the quantity of equatorial subsurface temperature data is unlikely to increase substantially because the subsurface temperature observational network has reached a plateau. In our investigation, there was no assimilation of surface fresh-water flux and subsurface salinity measurements, which preliminary tests have shown to be beneficial (Murtugudde and Busalacchi, 1997; Reynolds et al., 1997). Salinity measurements from a composite TAO and ship-of-opportunity network and satellite measurements of rainfall have the potential to reduce the salinity-related uncertainty of simulated fields. Excellent coverage in space and time of sea surface height variations are available from satellite altimetry measurements, which improve the representation of submonthly thermocline fluctuations (Carton et al., 1996). In the near-equatorial zone where geostrophic adjustment is weak, assimilation of velocity data would be helpful, especially in the eastern Pacific (Hao and Ghil, 1994). It is doubtful that, in the foreseeable future, there will be a sufficient quantity of vertical profiles of current measurements available for assimilation. However, near-surface (≈ 15-m depth) currents determined from satellite-tracked drifters are plentiful and have not yet been assimilated, which, as suggested by Anderson et al. (1996), may prove beneficial in the near-equatorial zone to initialize the velocity field of ubiquitous Kelvin waves.

The winds we employed were not optimum because all TAO wind measurements had not reached NCEP via the GTS in order for NCEP to insert TAO winds into the operational wind analyses. A composite NCEP and TAO wind product, named NCEP+TAO, had eastward zonal wind stress west of 170°E where the NCEP zonal wind stress was westward (Figure 6). East of the date line, the NCEP westward wind stress was smaller than that computed with NCEP+TAO data, with a 25% mean difference in the central Pacific (Figure 6). With NCEP+TAO winds, the mean EUC core speed simulated without data assimilation was not distinguishable from that computed with NCEP winds (not shown). However, with data assimilation the mean EUC core speeds in the eastern Pacific simulated with NCEP+TAO winds were 10- 15 cm s^{-1} smaller than those computed with NCEP winds (not shown). With the zonal gradient of the thermocline fixed by data assimilation, the NCEP+TAO westward wind stress apparently transferred more westward momentum to the ocean to reduce the EUC strength compared to that simulated with NCEP winds. If this mechanism was operative, there was no evidence in the SEC transports per unit width which, in the eastern Pacific, were the same for NCEP and NCEP+TAO wind data. In addition to improvements in the NCEP wind analyses, subdaily winds should be used to simulate subsurface oceanographic conditions because the heat flux is better represented (Rosati and Miyakoda, 1988). Subdaily winds had been available for our investigation but not used because the initial study had been performed with several monthly mean wind fields.

Parameterization of vertical mixing by turbulent processes can influence the impact of data assimilation. For instance, in the absence of data assimilation the Mellor and Yamada (1982) scheme yields a weaker EUC core speed in the eastern Pacific compared to that simulated with the Pacanowski and Philander (1981) method (Halpern et al., 1995). The choice of mixing parameterization would also influence the SEC, with deeper penetration of the SEC in the western Pacific produced by the Chen et al. (1994) mixing scheme compared to the NCEP version (Ji et al., 1995) of the Pacanowski and Philander (1981) method. Horizontal mixing also influences equatorial currents. A stronger EUC core speed would be expected by decreasing the intensity of horizontal mixing (Pacanowski and Philander, 1981), leading to a smaller effect produced by data assimilation. Studies of space- and time-dependent parametenzations of horizontal and vertical mixing are warranted.

Data assimilation in ocean models began about a decade ago, producing a suite of problems to solve, such as reduction of initialization shock. It is tempting to speculate that initialization shock, which excite erroneous motions in the process of velocity adjustment, would have a greater effect on simulated currents in the western Pacific than in the eastern Pacific because of the larger number of XBT profiles in the west. It was in the western equatorial Pacific that SEC simulations with and without data assimilation were quite different. Determining optimal assimilation methodology for climate prediction is current] y a topic of debate. As Malanotte-Rizzoli and Tziperman (1996, p. 13) stated in a review of the oceanographic data assimilation problem, "it is quite surprising to realize how much work is still required to meet" the objective of simulating ocean behavior in four dimensions. This is especially true for equatorial currents.

5 Acknowledgements

We are grateful to G. Eldin (ORSTOM), M. McPhaden (PMEL), and R. Weisberg (USF) for kindly sending current measurements from *l'Atalante*, from moored buoys at 165°E, 140°W and 110"W, and from the moored buoy at 170°W, respectively. Diagrams were prepared by K. Perry (JPL). The research described in this paper was performed, in part, by the Jet Propulsion Laboratory, California Institute of Technology, under contract with the National Aeronautics and Space Administration.

6 References

Acero-Schertzer, C. E., D. V. Hansen, and M. S. Swenson, 1997: Evaluation and diagnosis of surface currents in the National Centers for Environmental Prediction's ocean analyses. *J. Geophys. Res.*, 102, 21037-21048.

Anderson, D. L. T., J. Sheinbaum, and K. Haines, 1996: Data assimilation in ocean models. *Revs. Prog. Phys.*, *59*, *1209-1266.*

Cane, M. A., and E. S. Sarachik, 1979: Forced baroclinic ocean motion. 111. The linear equatorial basin case. *J. Mar. Res.*, 37, 355-398.

Carton, J. A., B. S. Giese, X. Cao, and L. Miller, 1996: Impact of altimeter, thermistor, and expendable bathythermograph data on retrospective analyses of the tropical Pacific Ocean. *J. Geophys. Res.*, 101, 14147-14159.

Chen, D., L. M. Rothstein, and A. J. Busalacchi, 1994: A hybrid vertical mixing scheme and its application to tropical ocean models. *J. Phys. Oceanogr.*, 24, 2156-2179.

Delcroix, T., G. Eldin, M. McPhaden, and A. Morliere, 1993: Effects of westerly wind bursts upon the western equatorial Pacific Ocean, February - April 1991. *J. Geophys. Res.*, 98, 16379-16385.

Eldin, G., M. Rodier and M.-H. Radenac, 1997: Physical and nutrient variability in the upper equatorial Pacific with westerly wind forcing and wave activity in October 1994. *Deep-Sea Res.,* in press.

Enfield, D. B., and J. E. Harris, 1995: A comparative study of tropical Pacific sea surface height variability: Tide gauges versus the National Meteorological Center data-assimilating ocean general circulation model, 1982-1992. *J. Geophys. Res.*, 100, 8661-8675.

Fukumori, I., 1995: Assimilation of TOPEX sea level measurements with a reduced-gravity, shallow water model of the tropical Pacific Ocean. *J. Geophys. Res.,* 100, 25027-25039.

Goddard, L., and N. E. Graham, 1997: El Niño in the 1990s. *J. Geophys. Res.,* 102, 10423-10436.

Gouriou, Y., and J. Toole, 1993: Mean circulation of the upper layers of the western equatorial Pacific Ocean. *J. Geophys. Res.*, 98, 22495-22520.

Halpern, D., Y. Chao, C.-C. Ma, and C. R. Mechoso, 1995: Comparison of tropical Pacific temperature and current simulations with two vertical mixing schemes embedded in an ocean general circulation model and reference to observations. *J. Geophys. Res.*, *100,* 2515-2522.

Hanawa, K., P. Rual, R. Bailey, A. Sy, and M. Szabados, 1995: A new depth-time equation for Sippican or TSK T-7, T-6 and T-4 expendable bathythermographs (XBT). *Deep-Sea Res.,* 42, 1423-1451.

Hao, Z., and M. Ghil, 1994: Data assimilation in a simple tropical ocean model with wind stress errors. *J. Phys. Oceanogr.*, 24, 2111-2128.

Ji, M., and T. M. Smith, 1995: Ocean model response to temperature data assimilation and varying surface wind stress: Intercomparisons and implications for climate forecast. *Mon. Wea. Rev.,* 123, 1811-1821.

Ji, M., A. Leetmaa, and J. Derber, 1995: An ocean analysis system for seasonal to interannual climate studies. *Mon. Wea. Rev., 123, 460-481.*

Leetmaa, A., and M. Ji, 1989: Operational hindcasting of the tropical Pacific. *Dyn. Atmos. Oceans,* 13, 465-490.

Leetmaa, A., and M. Ji, 1996: Ocean data assimilation as a component of a climate forecast system. *Modern Approaches to Data Assimilation in Ocean Modeling,* P. Malanotte-Rizzoli, Ed., Elsevier, 271-293.

Malanotte-Rizzoli, P., and E. Tziperman, 1996: The oceanographic data assimilation problem: Overview, motivation and purposes. *Modern Approaches to Data Assimilation in Ocean Modeling*, P. Malanotte-Rizzoli, Ed., Elsevier, 3-17.

McPhaden, M. J., 1995: The Tropical Atmosphere-Ocean array is completed. *Bull., Amer. Meteor. Sot., 76, 739-741.*

Mellor, G. L., and T. Yamada, 1982: Development of a turbulence closure model for geophysical fluid problems. *Rev. Geophys.*, 20, 851-875.

Murtugudde, R., and A. J. Busalacchi, Salinity effects in a tropical ocean model. *J. Geophys. Res.*, in press.

Pacanowski, R. C., and S. G. H. Philander, 1981: Parameterization of vertical mixing in numerical models of tropical oceans. *J. Phys. Oceanogr., 11,* 1443-1451.

Philander, S. G. H., W. Hurlin, and A. D. Seigel, 1987 A model of the seasonal cycle in the tropical Pacific Ocean. *J. Phys. Oceanogr.*, 17, 1986-2002.

Philander, S. G. H., D. Halpern, D. Hansen, R. Legeckis, L. Miller, C. Paul, R. Watts, R. Weisberg, and M. Wimbush, 1985: Long waves in the equatorial Pacific Ocean. *Eos, Trans. Amer. Geophys. Un., 66, 154.*

Plimpton, P. E., H. P. Freitag, and M J. McPhaden, 1997: ADCP velocity errors from pelagic fish schooling around equatorial moorings. *J. Atmos. Oceanic Tech.,* in press.

Reynolds, R. W., M. Ji, and A. Leetmaa, 1997, Use of salinity to improve ocean modeling. *Phys. Chem. Earth,* in press.

Rosati, A., and K. Miyakoda, 1988: A general circulation model for upper ocean simulation. *J. Phys. Oceanogr., 18, 1601-1626.*

Schopf, P. S., and A. Loughe, 1995: A reduced-gravity isopycnal ocean model: Hindcasts of El Niño. *Mon. Wea. Rev.,* 123, 2839-2863.

Weisberg, R. H., and C. Wang, 1997: Slow variability in the equatorial west-central Pacific in relation to ENSO. *J. Clim.*, *10*, 1998-2017.

Wijesekera, H. W., and M. C. Gregg, 1996: Surface layer response to weak winds, westerly bursts, and rain squalls in the western Pacific warm pool. *J. Geophys. Res.*, **101**, 977-997.

List of Figures

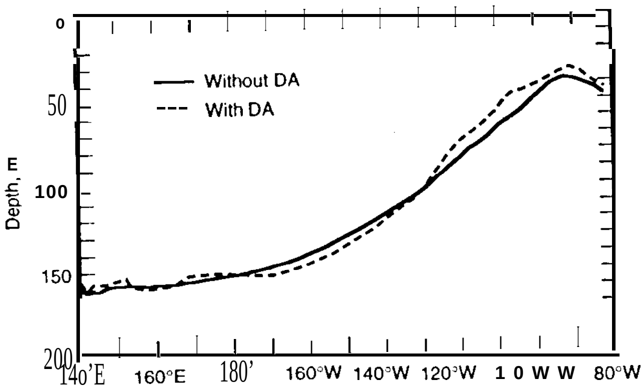
0
50
100
150
200
Depth, m
Without DA
With DA
140'E
160°E
180'
160°W
140°W
120°W
1 0 W W
80°W

Figure 1

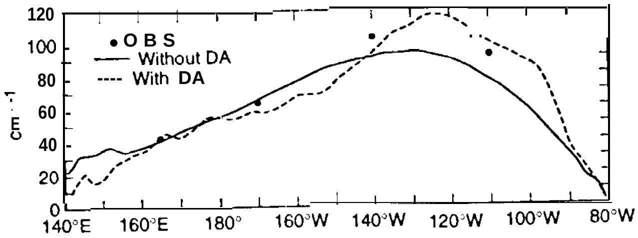

120
100
80
60
40
20
0
cm
O B S
Without DA
With DA
140°E
160°E
180°
160°W
140°W
120°W
100°W
80°W

Figure 2

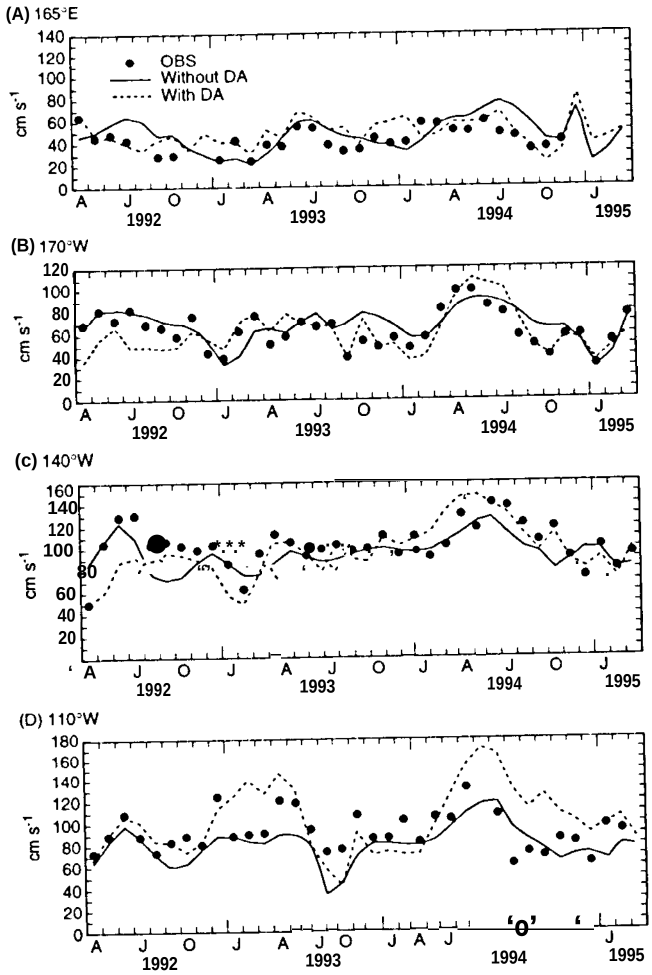
(A) 165°E
OBS
Without DA
With DA
cm s-1
A J O J A J O J A J O J
1992
1993
1994
1995
(B) 170°W
(c) 140°W
(D) 110°W

Figure 3

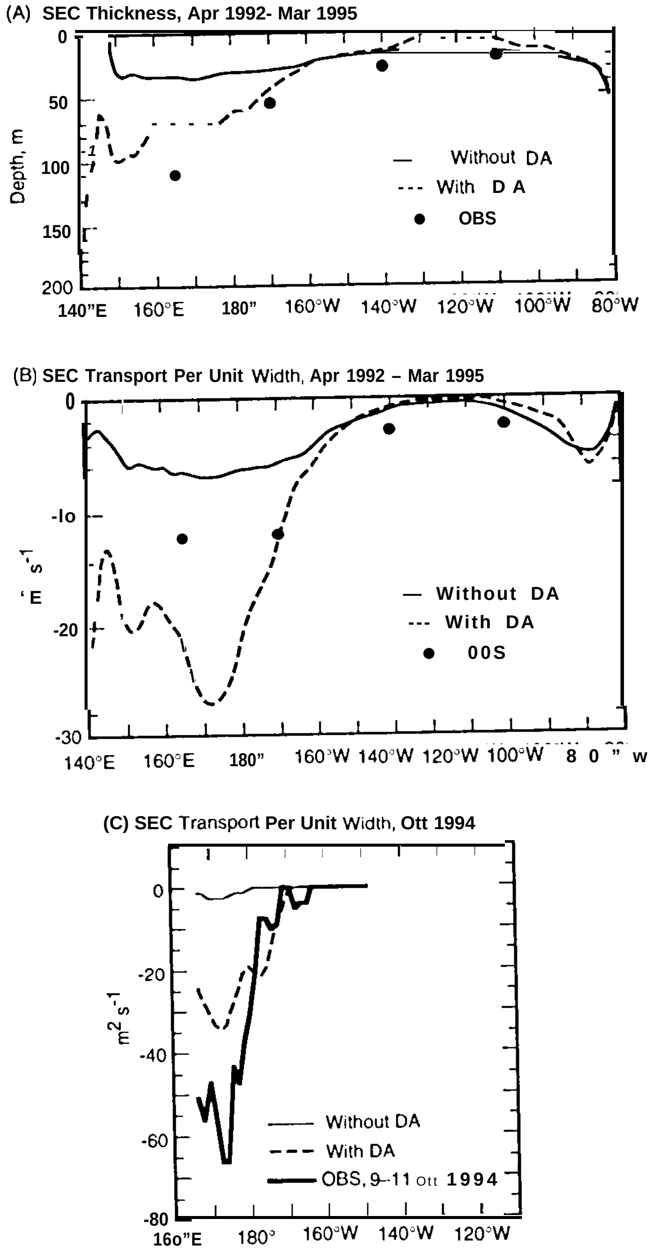

(A) SEC Thickness, Apr 1992- Mar 1995
Depth, m
0
50
100
150
200
140"E 160°E 180" 160°W 140°W 120°W 100°W 80°W
Without DA
With D A
OBS
(B) SEC Transport Per Unit Width, Apr 1992 – Mar 1995
0
-lo
-20
-30
140°E 160°E 180" 160°W 140°W 120°W 100°W
Without DA
With DA
00S
(C) SEC Transport Per Unit Width, Ott 1994
0
-20
-40
-60
-80
$m^2 s^{-1}$
160"E 180° 160°W 140°W 120°W
Without DA
With DA
OBS, 9–11 Ott 1994

Figure 4

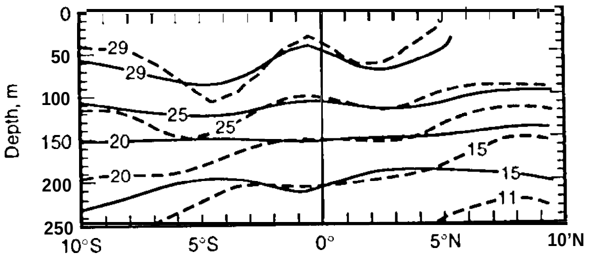

Depth, m
0
50
100
150
200
250
10°S
5°S
0°
5°N
10'N
29
29
25
25
20
20
15
15
11

Figure 5

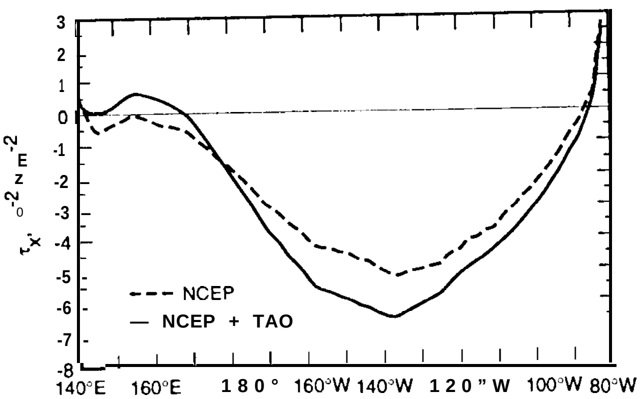

3
2
1
0
-1
-2
-3
-4
-5
-6
-7
-8
NCEP
NCEP + TAO
140°E
160°E
180°
160°W
140°W
120"W
100°W
80°W

Figure 6